Modeling and Designing a Hydrostatic Transmission With a Fixed-Displacement Motor

N. D. Manring
Department of Mechanical and Aerospace Engineering, University of Missouri-Columbia, Columbia, MO 65211

G. R. Luecke
Department of Mechanical Engineering, Iowa State University, Ames, IA 50011

This study develops the dynamic equations that describe the behavior of a hydrostatic transmission utilizing a variable-displacement axial-piston pump with a fixed-displacement motor. In general, the system is noted to be a third-order system with dynamic contributions from the motor, the pressurized hose, and the pump. Using the Routh-Hurwitz criterion, the stability range of this linearized system is presented. Furthermore, a reasonable control-gain is discussed followed by comments regarding the dynamic response of the system as a whole. In particular, the varying of several parameters is shown to have distinct effects on the system rise-time, settling time, and maximum percent-overshoot.

Introduction

Hydrostatic transmissions are used to transmit rotating mechanical-power from one source to another without the use of gears. One advantage of such a transmission is that the transfer of power can be accomplished on a variable basis, i.e., the transmission is not constrained by a finite number of gear-ratios. For this reason these transmissions are often referred to as "continuously-variable transmissions." Furthermore, hydrostatic transmissions can be used to transmit power in applications where the design of a gear train may be undesirable or impossible. It is often much easier to route a hydraulic hose through a machine than it is to establish the hard mesh of gears. There are also several disadvantages associated with hydrostatic transmissions. In particular, the transmission of power using a hydrostatic transmission is much less efficient than when using a set of gears for the same task. Second, hydrostatic transmissions provide a much "softer" transmission of power than a mechanical gear train. When considering the use of a hydrostatic transmission the dynamic contribution of the transmission must be considered whereas with a gear train such consideration is often not necessary.

Traditional research associated with hydrostatic transmissions has been conducted on a macroscopic level without a clear understanding of the dynamics associated with each component (Thoma, 1979; Merritt, 1967). Primarily, these studies have neglected to include the appropriate dynamics of the swash-plate control for the variable-displacement axial-piston pump. Until recently, little has been known about the driving forces of the swash plate itself in open literature and, perhaps, Zeiger and Akers (1985) are to be credited for the pioneering work in this area. Since the work of Zeiger and Akers, other research regarding the dynamics and control of the swash plate has appeared in the literature (Manring and Johnson, 1994; Schoenau et al., 1990; Kim et al., 1987; Zeiger and Akers, 1986). All of this work has contributed to a better understanding of the variable-displacement pump and to a better understanding of the hydrostatic transmission as a whole.

A linear model of the hydrostatic transmission is presented here. The importance of this model is that it now includes a better representation of the pump dynamics than previous research has been able to do. Furthermore, this model does not require the input of empirical test-data and all modeling parameters can be deduced from the geometry of the transmission design. This aspect of the model is critical for a priori analysis and lends itself to being useful for the up-front design of the transmission.

This study begins by developing the equations that describe the dynamics of the motor, the pressurized hose, and the pump. These three contributors are shown to produce a third-order linear system with stability limits that can be discussed using the Routh-Hurwitz stability criterion. Using simplified forms of the model, reasonable controller-design is then discussed and followed by comments regarding the effects of parameter variations on the overall system-response.

Figure 1 shows the schematic of the hydrostatic transmission that is modeled in this research. It should be noted that the input speed of the pump, ω_p, is constant and the output speed of the motor, ω_m, is variable. Furthermore, the low-pressure side of the system, P_o, is also considered to be constant while the high-pressure side, P_h, is modeled dynamically. In practice, this scenario is generally true as an auxiliary pump and a relief valve are typically used to maintain the constant pressure in the low-pressure line. Lastly, while the displacement of the motor is held constant, the displacement of the pump is continuously regulated by the pump swash-plate angle, α.

Derivation of Dynamic Equations

Motor Analysis. The motor shaft-speed, ω_m, of the hydrostatic transmission changes as a function of the system inertia and the applied torque to the driving shaft. Using Newton's second law this relationship is written,

$$I\dot{\omega}_m = T_{th} - T_{\text{load}}, \tag{1}$$

where T_{th} is the theoretical hydraulic-torque input to the motor and T_{load} is the torque exerted on the shaft by the load that the motor is trying to drive. From standard handbooks it can be shown that

$$T_{th} = V_m(P_h - P_o), \tag{2}$$

where V_m is the displacement of the motor, and P_h and P_o are the pressures on the high and low-pressure sides of the motor respectively. For this analysis, T_{load} will be considered a constant. Using Eqs. (1) and (2), the final equation describing the output speed of the motor is given by

$$\dot{\omega}_m = \frac{V_m}{I} P_h - \frac{V_m P_o + T_{\text{load}}}{I}. \tag{3}$$

Contributed by the Dynamic Systems and Control Division for publication in the JOURNAL OF DYNAMIC SYSTEMS, MEASUREMENT, AND CONTROL. Manuscript received by the DSCD October 12, 1995. Associate Technical Editor: R. S. Chandran.

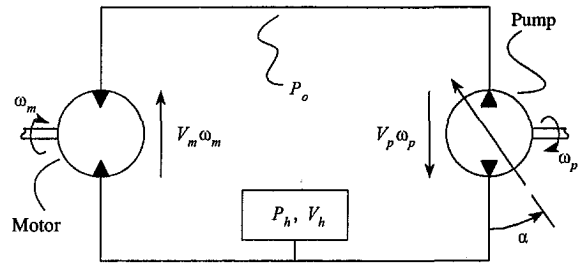

Fig. 1 Hydrostatic-transmission schematic

Hose Pressure. From the principles of mass conservation and the definition of the fluid bulk-modulus, the equation describing the pressure-rise rate within the system hose can be written as

$$\dot{P}_h = \frac{\beta}{V_h} Q_h, \tag{4}$$

where β is the fluid bulk-modulus, V_h is the volume of the hose, and Q_h is the net flow into the hose. Clearly, if we ignore all leakage effects the net flow into the hose may be expressed as

$$Q_h = V_p\omega_p - V_m\omega_m, \tag{5}$$

where V_p is the instantaneous displacement of the pump. Since ω_p is a constant, and knowing that the displacement of the pump is, linearly speaking, proportional to the swash-plate angle, α, we can write

$$V_p\omega_p = G_p\alpha, \tag{6}$$

where G_p is the pump-displacement gain. Using Eqs. (4), (5), and (6), the result for the pressure-rise rate within the hose may be expressed as

$$\dot{P}_h = \frac{\beta}{V_h} G_p\alpha - \frac{\beta}{V_h} V_m\omega_m. \tag{7}$$

Pump Analysis. Figure 2 shows a diagram of forces on the swash plate of the variable-displacement pump as its displacement is being regulated in a positive direction. The angle of the swash plate, α, is controlled with a hydraulic servo-system that is attached to the swash plate by a mechanical arm of length L. The forces of the servo system are resisted by a naturally-induced torque on the swash plate, T, that results from the pumping action of the pump itself. Since it has previously been shown that the inertia of the swash plate is negligible compared to the stiffness of the servo system (Kim et al., 1987; Zeiger and Akers, 1986), the moments on the swash plate can be

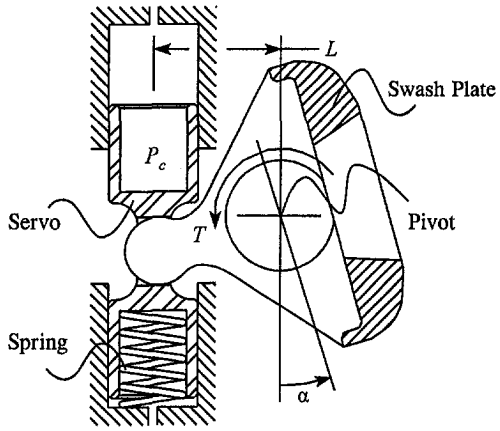

Fig. 2 Diagram of forces on the swash plate

statically summed to yield the following equation that governs the behavior of the swash-plate angle, α,

$$0 = T - F_{sp}L + A_sLP_c. \tag{8}$$

In Eq. (8), A_s is the area of the pressurized servo, P_c is the controlled pressure within this servo, and F_{sp} is the compressed-spring force within the opposite servo which is open to atmospheric pressure (i.e., zero gauge pressure).

The naturally induced torque on the swash plate, T, has been a topic of considerable research within the past ten years. Zeiger and Akers (1985) were the first to develop a numerical solution for this torque; however, Manring and Johnson (1994) later derived a closed-form approximation for this same torque and empirically verified the results. A linearized version of this closed-form result is given by

$$T = K_i\alpha - K_p(P_h - P_o). \tag{9}$$

The first term in Eq. (9) represents an inertial effect within the pump that tries to increase the stroke of the swash plate. The coefficient of this term, K_i, is given by

$$K_i = \frac{NM_pr^2\omega_p^2}{2}, \tag{10}$$

where N is the total number of pistons within the pump, M_p is the mass of a single piston, r is the piston pitch-radius, and ω_p is the constant input-speed of the pump.

The second term in Eq. (9) represents a pressure effect within the pump that tries to reduce the stroke of the swash plate. This term is strictly a result of the pressure carry-over on the valve plate which is discussed at length in previous work (Manring

Nomenclature

A_p = area of a single pump-piston
A_s = area of the servo
F_{sp} = swash-plate spring force
F_{sp_o} = reference swash-plate spring force
G_p = pump-displacement gain
G_s = control gain
I = system mass moment-of-inertia
K_i = coefficient of inertial swash-plate torque
K_p = coefficient of pressure swash-plate torque
k = spring constant
L = swash-plate arm length
M_p = mass of a single pump-piston
N = number of pistons within the pump
P_c = control pressure
P_h = dynamic hose-pressure
P_o = constant hose-pressure
Q_h = flow into the hose
Q_s = flow into the servo
r = pump piston-pitch radius
T = swash-plate torque
T_{load} = torque load on the motor shaft
T_{th} = theoretical hydraulic-torque
t = time
t_r = system rise-time
t_s = system settling-time
V_h = hose volume
V_m = motor volumetric-displacement
V_p = pump volumetric-displacement
V_s = servo volume
V_{s_o} = nominal servo-volume
α = pump swash-plate angle
β = fluid bulk-modulus
γ = pump pressure carry-over angle
ϵ = system error
λ = system eigenvalue
ω_m = motor shaft-speed
ω_o = desired motor shaft-speed
ω_p = pump shaft-speed

and Johnson, 1994). For the purposes of this research, the coefficient, K_p, will simply be presented here as

$$K_p = \frac{NA_p r\gamma}{2\pi}, \tag{11}$$

where A_p is the area of a single piston within the pump, and γ is the pressure carry-over angle on the valve plate. The pressure carry-over angle, γ, is a complicated quantity and generally requires numerical investigation for accurate prediction (though approximate closed-form solutions have been published). For the purposes of this research, γ will be considered a constant with reasonable values ranging between 0 and 0.42 radian (24°).

Equation (9) is a closed-form approximation of a very complicated phenomenon. By using this approximation it is now possible to accurately investigate an entire hydrostatic transmission in a closed form. Due to the complexity of the torque exerted on the swash plate, previous research has required the use of numerical techniques for the accurate modeling of any system using a variable displacement axial-piston hydrostatic pump. The advantages of closed-form modeling are obvious since linear analysis techniques may be employed and a physical understanding of the system may be determined without numerical iterations. To verify Eq. (9) an actual pump was tested and the results are presented in Figs. 4 and 5. See the Appendix.

The control pressure, P_c, of Eq. (8) is described by an equation similar to that of Eq. (4); however, the change in servo volume, V_s, must now be considered. The rise rate of this pressure is then given by

$$\dot{P}_c = \frac{\beta}{V_{s_o}}(Q_s - \dot{V}_s), \tag{12}$$

where, for mathematical expediency, the servo capacitance, β/V_{s_o}, is taken to be a constant. The net flow into the servo is given by Q_s and the instantaneous change in the volume of the servo is given by $\dot{V}_s$. The pump controller is used to direct flow in and out of the servo in a way that is proportional to some detected error, say, ϵ. In other words, the net flow into the servo is given by

$$Q_s = G_s\epsilon, \tag{13}$$

where G_s is the designed control-gain for the pump. The instantaneous volume of the servo is linearly expressed as

$$V_s = V_{s_o} + A_sL\alpha. \tag{14}$$

Using the results of Eqs. (12), (13), and (14), it can be shown that the control pressure within the servo is given by

$$P_c = \frac{\beta}{V_{s_o}} G_s \int \epsilon dt - \frac{\beta}{V_{s_o}}(A_sL)\alpha. \tag{15}$$

The spring force within the opposite servo also varies with the swash-plate angle. In general, this force may be expressed as

$$F_{sp} = F_{sp_o} + kL\alpha, \tag{16}$$

where F_{sp_o} is the spring force when the swash-plate angle is zero and k is the spring constant.

Substituting the results of Eqs. (9), (15), and (16) into Eq. (8), differentiating once with respect to time, using the result of Eq. (7), and dividing through by β/V_{s_o}, the time rate-of-change for the swash-plate angle may be expressed as

$$\dot{\alpha} = \frac{G_s(A_sL)\epsilon - \dfrac{V_{s_o}}{V_h}K_p(G_p\alpha - V_m\omega_m)}{(A_sL)^2 - \dfrac{V_{s_o}(K_i - kL^2)}{\beta}}. \tag{17}$$

Physically speaking, the denominator of Eq. (17) represents the stiffness of the swash plate servo-mechanism. By substituting reasonable values into the denominator of Eq. (17), it can be shown that $(A_sL)^2 \gg (V_{s_o}(K_i - kL^2)/\beta)$. This weighting of terms illustrates the fact that the stiffness of the swash plate servo-mechanism is dominated by the fluid bulk-modulus and that in comparison the spring and the inertial effects of the swash-plate torque are negligible. Therefore, neglecting the term that is inversely proportional to β, a simplified form of Eq. (17) may be written as

$$\dot{\alpha} = \frac{G_s}{(A_sL)}\epsilon - \frac{V_{s_o}}{V_h}\frac{K_p}{(A_sL)^2}(G_p\alpha - V_m\omega_m). \tag{18}$$

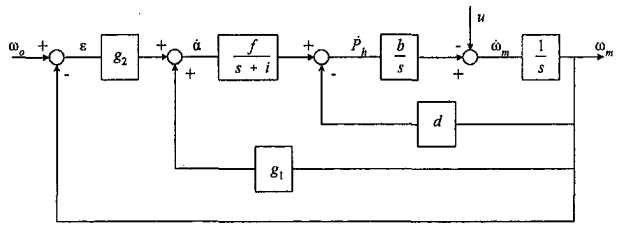

Fig. 3 Block diagram of the hydrostatic transmission

Dynamic Transmission Model

Generally, hydrostatic transmissions are used to provide a specific motor shaft-speed output, say, ω_o. In this case, the detected error of the system is given by

$$\epsilon = \omega_o - \omega_m. \tag{19}$$

Using this error definition, and Eqs. (3), (7), and (18), the dynamic system of the hydrostatic transmission may be expressed as

$$\begin{bmatrix} \dot{\omega}_m \\ \dot{P}_h \\ \dot{\alpha} \end{bmatrix} = \begin{bmatrix} 0 & b & 0 \\ -d & 0 & f \\ (g_1 - g_2) & 0 & -i \end{bmatrix}\begin{bmatrix} \omega_m \\ P_h \\ \alpha \end{bmatrix} + \begin{bmatrix} -u \\ 0 \\ w \end{bmatrix}, \tag{20}$$

where

$$b = \frac{V_m}{I}, \quad d = \beta\frac{V_m}{V_h}, \quad f = \beta\frac{G_p}{V_h}, \quad g_1 = \frac{V_{s_o}}{V_h}\frac{V_m}{(A_sL)^2}K_p,$$

$$g_2 = \frac{G_s}{(A_sL)}, \quad i = \frac{V_{s_o}}{V_h}\frac{G_p}{(A_sL)^2}K_p,$$

$$u = \frac{V_m}{I}P_o + \frac{T_{\text{load}}}{I}, \quad w = g_2\omega_o. \tag{21}$$

The block diagram for this system is shown in Fig. 3.

The transient response of the transmission is characterized by the system eigenvalues. These eigenvalues are determined by the solution to the characteristic equation which is given as

$$a_3\lambda^3 + a_2\lambda^2 + a_1\lambda + a_0 = 0, \tag{22}$$

where

$$a_3 = I, \quad a_2 = I\frac{V_{s_o}}{V_h}\frac{G_pK_p}{(A_sL)^2},$$

$$a_1 = \beta\frac{V_m^2}{V_h}, \quad a_0 = \beta\frac{V_m}{V_h}\frac{G_pG_s}{(A_sL)}. \tag{23}$$

Stability Criterion. The Routh-Hurwitz stability criterion may now be used to discuss the stability limits of the system. Since the coefficients of Eq. (22) are clearly positive, the remaining condition to be satisfied for guaranteed stability is that $a_1a_2 > a_0a_3$. More explicitly, this condition is expressed as

$$\frac{V_m}{V_h} > \frac{(A_s L)}{V_{s_o}} \frac{G_s}{K_p}. \tag{24}$$

The stability criterion presented in Eq. (24) describes the interaction of the speed at which the system eliminates the detected error and the degree to which the controller tries to compensate for this error. In essence, by increasing the displacement of the motor, V_m, or by decreasing the volume of the hose, V_h, the time rate-of-change for the motor speed and the system pressure increases, and tends to eliminate the detected error very quickly. This behavior improves the system stability. On the other hand, by making the control gain, G_s, too large the controller tends to overcompensate for the detected error and the system behaves in an unstable manner. Decreasing the servo volume, V_{s_o}, or increasing the length of the servo linkage, L, has the same effect as increasing the control gain, G_s.

Controller Design. For initial design purposes, it is helpful to have a criterion that establishes a reasonable design limit for the controller gain, G_s. If we temporarily ignore the inertial effects of the system (i.e., set $I = 0$), we can see from Eqs. (22) and (23) that the system becomes classified as a first-order system with a single eigenvalue

$$\lambda = \frac{-G_p G_s}{V_m (A_s L)}. \tag{25}$$

For good response, a typical design requires that the controller eliminate 98% of the detected error within a specified amount of time, say, t_s. Another way of saying this is to require the eigenvalue of Eq. (25) to be less than $-4/t_s$; or rather,

$$G_s > \frac{4}{t_s} \frac{V_m (A_s L)}{G_p}. \tag{26}$$

Using the results of Eqs. (24) and (26) it can be shown that reasonable design limits for the control gain, G_s, are given by

$$\frac{V_{s_o}}{V_h} \frac{V_m K_p}{(A_s L)} > G_s > \frac{4}{t_s} \frac{V_m (A_s L)}{G_p}. \tag{27}$$

Dynamic Response. Generally, the coefficient, a_3, of the characteristic equation presented in Eq. (22) is much, much smaller than the coefficients a_2, a_1, and a_0. This weighting of coefficients tends to produce solutions to Eq. (22) with a single real-root that lies to the far left-hand side of the real-imaginary plane and two complex conjugates that lie fairly close to the origin. Physically speaking, this scenario describes a third-order system that responds very much like a second-order system. By simply ignoring the first term in Eq. (22), the characteristic equation of the system can be approximated as

$$a_2 \lambda^2 + a_1 \lambda + a_0 = 0, \tag{28}$$

with eigenvalues given by

$$\lambda = \frac{-a_1 \pm \sqrt{a_1^2 - 4 a_2 a_0}}{2 a_2}. \tag{29}$$

The coefficients a_2, a_1, and a_0 are given in Eq. (23). These eigenvalues are comprised of a real part, $\mathcal{R}(\lambda)$, and an imaginary part, $\mathcal{I}(\lambda)$, and the dimensionless damping ratio for the system is

$$\zeta = \sqrt{\frac{1}{(\mathcal{I}(\lambda)/\mathcal{R}(\lambda))^2 + 1}}. \tag{30}$$

The most important response-characteristics of this system are the rise time, t_r, the settling time, t_s. and the maximum percent-overshoot. The rise time is defined as the amount of time required for the system to first reach 100% of its steady-state condition. To reduce the rise time, the absolute value of the imaginary part of the system eigenvalues, $\mathcal{I}(\lambda)$, must be increased. The settling time refers to the amount of time it takes for the system to arrive at, and stay within, 98 percent of the steady-state condition. The settling time is reduced by increasing the absolute value of the real part of the system eigenvalues, $\mathcal{R}(\lambda)$. The maximum percent-overshoot refers to the first peak of overshoot after the system has arrived at, and exceeded, 100 percent of the steady-state condition. To reduce the maximum percent-overshoot the damping ratio, ζ, must be increased.

Table 1 Effects on the system reponse when varying certain parameters

Parameter	t_r	t_s	Overshoot
$\delta I > 0$	+	+	No effect
$\delta V_{s_o} > 0$	+	+	+
$\delta G_p > 0$	Inconsistent	+	+
$\delta V_m > 0$	Inconsistent	−	Inconsistent
$\delta G_s > 0$	−	No effect	+
$\delta L > 0$	Inconsistent	−	−

Based upon a closed-form investigation of the system eigenvalues, Table 1 illustrates changes in system response-characteristics that can be expected when various parameters are increased. For instance, from Table 1 it can be seen that by increasing the control gain, G_s, the system rise-time is reduced (−), the system settling-time is unaffected (no effect), and the maximum percent-overshoot is increased (+). Conversely, it should be assumed that by *decreasing* this same parameter an opposite effect would be exhibited for the rise time and the settling time. When a parameter variation is said to be "inconsistent," that means that the effect of this variation may change depending upon other design characteristics of the transmission (i.e., a consistent statement cannot be made for all transmission designs).

Conclusion

In this research, the dynamic model of a hydrostatic transmission has been derived. Based upon this model, the stability of the system has been discussed and shown to be a result of the speed at which the system tries to eliminate the detected error and the degree to which the controller tries to compensate for this error. An overcompensating control or an extremely slow-responding system has been shown to result in an unstable transmission-design. Furthermore, based upon the Routh-Hurwitz stability criterion and a simplified model of the transmission system, a range of reasonable design-limits for the controller gain has been presented in equation (27). In this study, it was also recognized that two complex roots of the transmission's characteristic equation lie near the origin of the real-imaginary plane while the third root, which is real, lies to the far left of the same origin. This scenario describes a third-order system that behaves much like a second-order system. Based upon a second-order approximation of the characteristic equation, the effect of particular design variations on the system rise-time, settling time, and maximum percent-overshoot has been tabulated in Table 1. Overall, this study has provided greater insight into the behavior of a hydrostatic transmission and has given the designer of these same machines a tool that is useful for analyzing the response of the transmission before it is actually built.

References

Kim, S. D., H. S. Cho, and C. O. Lee, 1987, "A Parameter Sensitivity Analysis for the Dynamic Model of a Variable Displacement Axial Piston Pump," *Proceedings of the Institution of Mechanical Engineers,* Vol. 201, No. C4:235–43.

Manring, N. D., and R. E. Johnson, 1994, "Swivel Torque within a Variable-Displacement Pump," 46th National Conference on Fluid Power, Anaheim, CA.

Merritt, Herbert E., 1967, *Hydraulic Control Systems,* Wiley, New York.

Schoenau, G. J., R. T. Burton, and G. P. Kavanagh, 1990, "Dynamic Analysis of a Variable Displacement Pump," ASME JOURNAL OF DYNAMIC SYSTEMS, MEASUREMENT, AND CONTROL, Vol. 112, pp. 122–32.

Thoma, Jean U., 1979, *Hydrostatic Power Transmission,* Trade and Technical Press, Surrey, England.

Zeiger, G., and Akers, 1986, "Dynamic Analysis of an Axial Piston Pump Swashplate Control," *Proceedings of the Institution of Mechanical Engineers,* 200, No. C1. pp. 49–58.

Zeiger, G., and Akers, 1985, "Torque on the Swashplate of an Axial Piston Pump," ASME JOURNAL OF DYNAMIC SYSTEMS, MEASUREMENT, AND CONTROL, Vol. 107, pp. 220–26.

APPENDIX

This appendix presents the experimental results that were obtained in an effort to validate Eq. (9). In the laboratory, a 215 cc/rev variable displacement pump was instrumented and

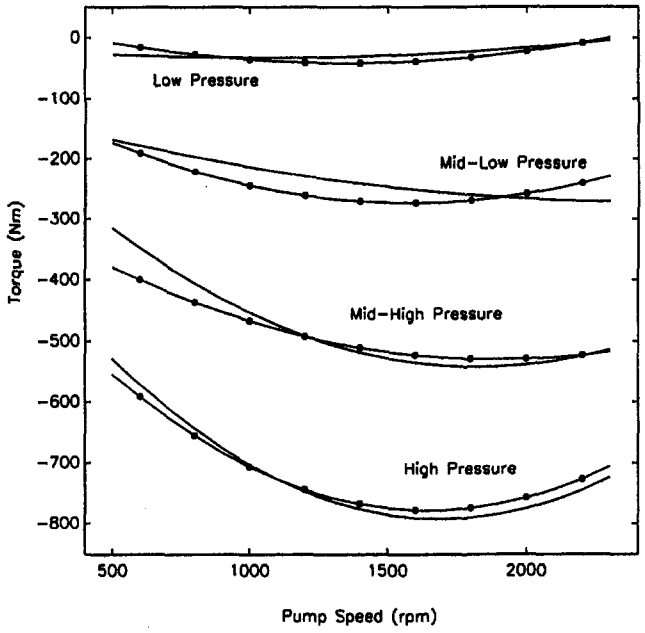

Fig. 4 Torque for low swash-plate angles

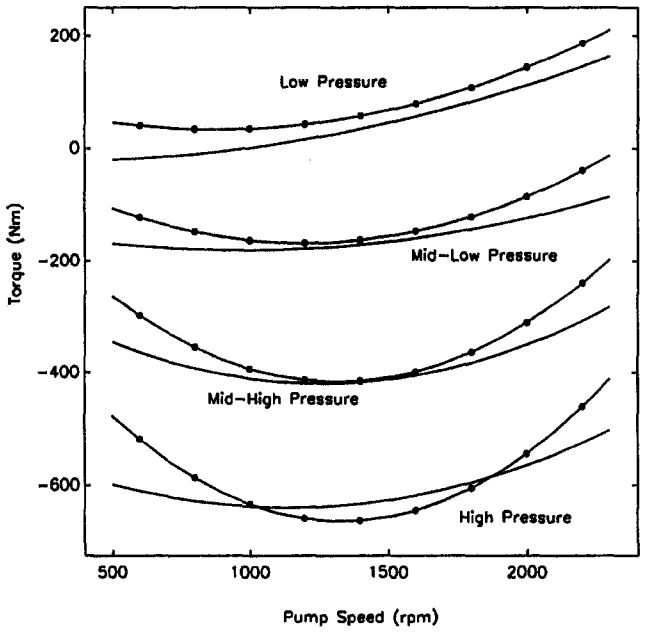

Fig. 5 Torque for high swash-plate angles

operated at various shaft speeds, discharge pressures, and two swash-plate angles. For steady-state operation, the control pressure, P_c, of Eq. (8) was measured and the spring force, F_{sp}, was calculated using Eq. (16). Using these results and Eq. (8) the torque, T, was calculated and compared with the predicted results of Eq. (9). This comparison is presented in Figs. 4 and 5 and the correlation between theoretical and experimental data is shown to be good. In Figs. 4 and 5, the lines with circles represent test data while the lines without circles represent theoretical expectations. A negative value of torque corresponds with a stroke decreasing influence while a positive value of torque corresponds with a stroke increasing effect. This sign convention is consistent with Eq. (9). Note: for a full derivation of Eq. (9) the reader is referred to the paper by Manring and Johnson (1994).